Supporting Material

Title: Spatial Dynamics of Multi-stage Cell Lineages in Tissue Stratification

Authors: Ching-Shan Chou, Wing-Cheong Lo, Kimberly K. Gokoffski, Yong-Tao Zhang, Frederic Y.M. Wan, Arthur D. Lander, Anne L. Calof, and Qing Nie

Supporting Information

Spatial Dynamics of Multi-stage Cell Lineages in Tissue Stratification

Ching-Shan Chou[5], Wing-Cheong Lo[1,2], Kimberly K. Gokoffski[1,4], Yong-Tao Zhang[6], Frederic Y.M. Wan[1,2], Arthur D. Lander[1,3], Anne L. Calof[1,4], and Qing Nie[1,2]

[1]Center for Complex Biological Systems
[2]Department of Mathematics
[3]Department of Developmental and Cell Biology
[4]Department of Anatomy and Neurobiology
University of California at Irvine, Irvine, CA 92697, USA

[5]Department of Mathematics
The Ohio State University, Columbus, OH 43210, USA

[6]Department of Applied and Computational Mathematics and Statistics
University of Notre Dame, Notre Dame, IN 46556, USA

Corresponding author: Ching-Shan Chou (chou@math.ohio-state.edu)

CONTENTS OF THIS SUPPLEMENT

I. MATERIAL AND METHODS

A. Numerical method to solve Eqs. 1-8 with a quasi-steady-state approximation of the molecule actions

A.1. *A linear model assuming the abundance of receptors*

To describe the dynamics of molecules *A* and *G* within a tissue, we use a model in Eqs. **6**-**7** (repeated in Eqs. **S1**-**S2** for clarity of explanation), where diffusion of those molecules are described by the effective diffusion rates D_A and D_G respectively; the removal of molecules due to degradation or binding with other molecules are controlled by rate constants $a_{\mathrm{deg}}, g_{\mathrm{deg}}$; the synthesis of *A* and *G* are assumed to be proportional to the density of each cell type that produces them with rates μ_j and η_j, as η_0 being zero to reflect the fact *G* is only produced by TA and TD cells. Then we obtain the concentration of *A* and *G* within the tissue $(0, z_{\max})$:

$$\frac{\partial [A]}{\partial t} + \frac{\partial (V[A])}{\partial z} = D_A \frac{\partial^2 [A]}{\partial z^2} + \sum_{j=0}^{2} \mu_j C_j - a_{\mathrm{deg}}[A], \qquad \textbf{[S1]}$$

$$\frac{\partial [G]}{\partial t} + \frac{\partial (V[G])}{\partial z} = D_G \frac{\partial^2 [G]}{\partial z^2} + \sum_{j=0}^{2} \eta_j C_j - g_{\mathrm{deg}}[G]. \qquad \textbf{[S2]}$$

Here, the convection term is due to growth of the tissue. The uptake of *A* and *G* due to leakage and binding with other molecules in the underlying stroma are modeled in Eq. **8**, and no-flux conditions are imposed for both *A* and *G* at $z = z_{\max}$.

The typical time scales of cell cycle lengths and tissue growth of OE and other similar systems are days, whereas those for molecule interactions are hours. The morphogen system quickly reaches steady state within the time scale of cell cycle lengths, and therefore we use quasi-steady-state approximation for Eqs. **S1**-**S2**:

$$0 = D_A \frac{\partial^2 [A]}{\partial z^2} + \sum_{j=0}^{2} \mu_j C_j - a_{\mathrm{deg}}[A] \qquad \textbf{[S3]}$$

$$0 = D_G \frac{\partial^2 [G]}{\partial z^2} + \sum_{j=0}^{2} \eta_j C_j - g_{\mathrm{deg}}[G] \qquad \textbf{[S4]}$$

$$\frac{\partial [G]}{\partial z}(0) = \alpha_G [G], \quad \frac{\partial [A]}{\partial z}(0) = \alpha_A [A], \qquad \textbf{[S5]}$$

To solve this system, we first transform Eqs. **1**-**4**, **S3**-**S5** by scaling z with $z_{\max}$ such that the new spatial variable is in a fixed domain [0,1] and the dynamics of $z_{\max}$ is embedded in the coefficients of the transformed PDEs. The corresponding equations for **S3**-**S5** are then solved using a multigrid method (1) with the Laplacian approximated by a second order central difference method. Eqs. **1**-**3** are then solved using upwind scheme with appropriate boundary conditions, while the temporal discretization is carried out using a fourth order Adams-Moulton predictor-corrector method. Eq. **4** is integrated with the trapezoidal rule.

A typical number of spatial grid points used in the simulations was 512 with a time-step size 10^{-4}. We tested a range of grid and time-step sizes to assure convergence of the numerical

solutions.

A.2. *A nonlinear model with receptor-ligand binding*

Biochemical evidence suggests that the secreted TGF-β's have long half-lives and may not undergo simple linear decay during tissue growth. Instead, the ligands bind available receptors that are endocytosed leading to the removal of ligands from the extracellular pool. If the receptors are not saturated in the given range for GDF11 and ActivinβB, linear degradation of those molecules may be appropriate to describe their removal, as in A.1, but if the receptors are saturated, the degradation becomes nonlinear. Here we explore the possibility of saturated receptors by explicitly including in the equations: 1) free GDF11 molecule, 2) receptor-bound GDF11, 3) free ActivinβB molecule, and 4) receptor-bound ActivinβB molecule, while assuming the total numbers of GDF11 receptors R_G and ActivinβB receptors R_A are constants. The system then is described by the following equations:

$$\frac{\partial [A]}{\partial t} + \frac{\partial (V[A])}{\partial z} = D_A \frac{\partial^2 [A]}{\partial z^2} + \sum_{j=0}^{2} \mu_j C_j - \sigma_A [A](R_A - [AR]) + \beta_A [AR],$$

$$\frac{\partial [G]}{\partial t} + \frac{\partial (V[G])}{\partial z} = D_G \frac{\partial^2 [G]}{\partial z^2} + \sum_{j=0}^{2} \eta_j C_j - \sigma_G [G](R_G - [GR]) + \beta_G [GR],$$

$$\frac{\partial [AR]}{\partial t} + \frac{\partial (V[AR])}{\partial z} = \sigma_A [A](R_A - [AR]) - \beta_A [AR] - a_{\deg}[AR],$$

$$\frac{\partial [GR]}{\partial t} + \frac{\partial (V[GR])}{\partial z} = \sigma_G [G](R_G - [GR]) - \beta_G [GR] - g_{\deg}[GR],$$

Similar as in A.1, due to the different time scales of cell cycle lengths and of the molecule interactions, we use the quasi-steady-state approximations for this system:

$$0 = D_A \frac{\partial^2 [A]}{\partial z^2} + \sum_{j=0}^{2} \mu_j C_j - a_{\deg}[AR],$$

$$0 = D_G \frac{\partial^2 [G]}{\partial z^2} + \sum_{j=0}^{2} \eta_j C_j - g_{\deg}[GR],$$

$$[AR] = R_A \frac{[A]}{[A] + K_A},$$

$$[GR] = R_G \frac{[G]}{[G] + K_G}.$$

where $K_A = \dfrac{\beta_A + a_{\deg}}{\sigma_A}$, and $K_G = \dfrac{\beta_G + g_{\deg}}{\sigma_G}$ are half-maximal constants for $[AR]$ and $[GR]$.

The boundary conditions of A and G are

$$\frac{\partial[G]}{\partial z}(0) = \alpha_G[G], \quad \frac{\partial[A]}{\partial z}(0) = \alpha_A[A].$$

Since now it is the receptor-bound ligand that inhibits the cell proliferation, we replace Eq. **5** by

$$p_0 = \frac{\bar{p}_0}{1 + (\gamma_A[AR])^m}, \quad p_1 = \frac{\bar{p}_1}{1 + (\gamma_G[GR])^n}.$$

We numerically solve the above system for the steady state solution using two sets of parameters representing two typical cases: high saturated receptors and low saturated receptors. The parameters are listed in Tables S1 and S3. For simplicity, we take R_A and R_G in our model to be 1, and hence $[AR]$ and $[GR]$ are between 0 and 1. We choose the highly saturated receptors to have the ligand-binding proportion higher than 0.5, and the low saturated receptors have the proportion lower than 0.5. In Fig. S1A, a highly saturation case, the spatial distributions of $[A]$ and $[AR]$ are different, indicating the saturation of the receptors. In Fig. S1B, a low saturation case, the spatial distributions of $[A]$ and $[AR]$ are similar, showing linear relationship between these quantities. This case corresponds to the one in A.1 which approximates the removal of $[A]$ as linear decay.

Although receptors may be highly saturated (Fig. S1A), $[AR]$ can exhibit a spatial gradient due to the leaky boundary. To compare the nonlinear model with the linear model in A.1, we perform similar calculations as shown in Fig. 3A. The simulation results (Fig. S1C) indicate that as the permeability increases, the tissue stratification measured by SF becomes larger and the epithelium becomes thicker, with similar magnitudes as in Fig. 3A, showing the linear and nonlinear models behave similarly.

II. RESULTS

A. Without feedback regulation on cell proliferation and the cell cycle lengths, $\bar{p}_0$ is required to be 0.5 for the system to reach a finite size with non-zero stem cell population, and the resulting cell distribution is uniform in space.

One of the most important performance objectives of tissues is to reach and maintain an appropriate size. To reach an appropriate homeostasis, the multi-stage cell lineage has to tightly control the proliferation of the cells. If one only considers the cell population in a homogenized, non-spatial setting, an ODE model similar to Eq. **1**-**3** (except that the variables are functions of only time and there are no convection terms) can be derived as in (2, 3). In those ODE models, it was analytically shown that if the replication probability of the stem cells is a constant, then it has to be exactly 0.5 for the system to reach a finite size with a non-zero stem cell population (2, 3). In other words, the stem cells have to undergo perfect asymmetric divisions, which does not normally happen. Here, we would like to show that this theoretical result is still true for our spatial model, and we will further show that the spatial distribution of the cells will be uniform if the stem cells undergo perfect asymmetric divisions, provided other cells also proliferate with constant probabilities.

We begin with defining the steady state of the system to be a state with the tissue size and local cell density at equilibrium ($\frac{\partial C_0}{\partial t} = \frac{\partial C_1}{\partial t} = \frac{\partial C_2}{\partial t} = 0, \ \frac{dz_{max}}{dt} = 0$). Note that in this definition,

we do not require $V(z,t) = 0$ for all z, but only at $z_{\max}$. It will be proved in A.2 that when p_0 is 0.5, the above definition implies $V(z,t) = 0$ for all z. In the following, we will prove two results in the subsections: in A.1, we show that without feedback regulation on proliferation, p_0 is required to be 0.5 for the system to reach a finite size with non-zero stem cell density; in A.2, we prove that given the assumptions and results in A.1, the cell distribution is uniform in space.

A.1. *Without feedback regulation on proliferation and the cell cycle lengths, $\bar{p}_0$ is required to be 0.5 for the system to reach a finite size with a non-zero stem cell population*

In order to obtain conditions on constants p_j, we remove the convection terms by defining new variables $\bar{C}_j(t) = \int_0^{z_{\max}(t)} C_j(z,t)\, dz$, $j = 0,1,2$. Using the fact that p_j and v_j are constants (no feedback regulation) and $V(0,t) = 0$, we obtain the following equations:

$$\frac{d\bar{C}_0}{dt} = v_0(2p_0 - 1)\bar{C}_0,$$ [S6]

$$\frac{d\bar{C}_1}{dt} = v_0\left[2(1 - p_0)\bar{C}_0\right] + v_1\left[(2p_1 - 1)\bar{C}_1\right],$$ [S7]

$$\frac{d\bar{C}_2}{dt} = v_1\left[2(1 - p_1)\bar{C}_1\right] - d_2\bar{C}_2.$$ [S8]

While $C_j(z,t)$ is defined as cell density, $\bar{C}_j$ can be interpreted as the total cell population of cell type j within the epithelium. Eqs. **S6**-**S8** are consistent with the non-spatial model in (2), where only cell populations are accounted for. By Eq. **S6**, a steady state with a non-zero stem cell population requires p_0 to be exactly 0.5 and $\bar{C}_0$ be constant at any time; by Eq. **S7**, p_1 is required to be strictly less than 0.5 to ensure a non-zero steady state of TA cells.

A.2. *Without feedback regulation on proliferation and the cell cycle lengths, the cell distribution is uniform in space*

With conditions $p_0 = 0.5$ and $p_1 < 0.5$ obtained in A.1, we can derive a system from Eqs. **1**-**3** for the steady states of C_0, C_1, C_2 and $V(z)$, denoted by $C_{0ss}(z)$, $C_{1ss}(z)$, $C_{2ss}(z)$ and $V_{ss}(z)$ respectively:

$$0 = -\frac{\partial(V_{ss}C_{0ss})}{\partial z},$$ [S9]

$$0 = -\frac{\partial(V_{ss}C_{1ss})}{\partial z} + v_0 C_{0ss} + v_1\left[(2p_1 - 1)C_{1ss}\right],$$ [S10]

$$0 = -\frac{\partial(V_{ss}C_{2ss})}{\partial z} + v_1\left[2(1 - p_1)C_{1ss}\right] - d_2 C_{2ss},$$ [S11]

$$\frac{\partial V_{ss}}{\partial z} = v_0 C_{0ss} + v_1\left[(2p_1 - 1)C_{1ss}\right] + v_1\left[2(1 - p_1)C_{1ss}\right] - d_2 C_{2ss},$$ [S12]

$$0 = V_{ss}(\bar{z}_{\max}),$$

where $\bar{z}_{\max}$ is the thickness of the tissue at the steady state.

After integrating Eq. **S9** from 0 to z, we obtain that $V_{ss}(z)C_{0ss}(z)$ is a constant within the epithelium. Since $V_{ss}(0)=0$, we have $V_{ss}(z)C_{0ss}(z)=0$ for all z in $[0,\bar{z}_{\max}]$. In the following, we show that $V_{ss}(z)=0$ for all z in $[0,\bar{z}_{\max}]$. Suppose $V_{ss}(z)$ is *not* entirely zero in $[0,\bar{z}_{\max}]$, by the continuity of V_{ss}, there exists an interval $[z_1,z_2]$ with $z_1 \neq z_2$ and $0 \leq z_1,z_2 \leq \bar{z}_{\max}$ such that V_{ss} is non-zero in the interval but $V_{ss}(z_1)=V_{ss}(z_2)=0$. By the condition $V_{ss}(z)C_{0ss}(z)=0$ for all z, one can obtain $C_{0ss}(z)=0$ in (z_1,z_2). Integrating Eqs. **S10**-**S11** from z_1 to z_2, we obtain

$$0 = v_1\left[(2p_1-1)\int_{z_1}^{z_2} C_{1ss}(z)\,dz\right], \tag{S13}$$

$$0 = v_1\left[2(1-p_1)\int_{z_1}^{z_2} C_{1ss}(z)\,dz\right] - d_2\int_{z_1}^{z_2} C_{2ss}(z)\,dz. \tag{S14}$$

With the assumption $p_1 < 0.5$, $\int_{z_1}^{z_2} C_{1ss}(z)\,dz$ must be zero by Eq. **S13** and this also implies that $\int_{z_1}^{z_2} C_{2ss}(z)\,dz = 0$ using Eq. **S14**. This contradicts the underlying relation $C_{0ss}(z)+C_{1ss}(z)+C_{2ss}(z)=1$. Therefore, $V_{ss}(z)$ must vanish everywhere. To prove the uniform distribution of the cells, we take Eqs. **S10**-**S11**, together with $V_{ss}(z)=0$ and the definition of $C_{jss}(z)$, and finally obtain

$$0 = v_0 C_{0ss}(z) + v_1\left[(2p_1-1)C_{1ss}(z)\right],$$
$$0 = v_1\left[2(1-p_1)C_{1ss}(z)\right] - d_2 C_{2ss}(z),$$
$$1 = C_{0ss}(z) + C_{1ss}(z) + C_{2ss}(z).$$

With constant parameters, this system is linear and has the same unique solution for all z. This proves that without any feedback, the spatial distribution of cells is always uniform.

B. Relation between the coefficients of permeability in Eq. 8 and the decay lengths of regulatory molecules *A* and *G*

Both in our modeled system and in OE, the epithelium is bounded atop by a layer of tightly packed sustentacular cells, preventing the epithelial regulatory molecules from escaping to the adjacent cavity. This diffusion barrier is modeled by no-flux boundary conditions at $z = z_{\max}$. On the other hand, the epithelium sits atop the basal lamina, a permeable membrane that allows molecules to diffuse through and bind with other molecules in the stroma. We model this permeability and the molecule uptake in the stroma by leaky boundary conditions in Eq. **8**, in which the coefficients stand for the level of permeability and the strength of the uptake. In this section, we explore physical meaning of permeability coefficients: *the ratio between decay lengths in the epithelium and the stroma*. Decay length typically describes average distance that a molecule travels before it is degraded. More precisely, if the molecule degrades with rate constant k and diffuses with rate D, the decay length can be formulated by $\sqrt{D/k}$. In the epithelium that we model, a diffusing regulatory molecule *A* or *G* may have different decay lengths at two sides of the basal lamina, due to its differential diffusion and degradation rates in

the epithelium and stroma.

In order to characterize the permeability coefficient, we consider a domain consisting of both epithelium ($0 < z < z_{max}$) and stroma ($z < 0$), with the basal lamina in between at $z = 0$ (in the main text, we only consider the epithelium, taking the basal lamina as a boundary). Here, we use a to denote the concentration of the diffusing regulatory molecule A or G. Let D stand for the diffusion coefficient of the molecule, and k be its degradation rate constant. Because D and k may be different in the epithelium versus the stroma, we use subscripts E and S to distinguish those rate constants in epithelial and stroma regions, respectively. By the fact that the regulatory molecules reach quasi steady-state under the time scale of cell cycle lengths, only the steady state distribution of a is considered. In this case, a only depends on the space variable z. In order to have boundary conditions at the two ends, we define a "dummy point" $-z_{min} < 0$, where we will set a to zero. In the solution, we take z_{min} as infinity, so that the result corresponds to an open-ended stroma. Since a represents the molecule A or G that is only produced in the epithelium, we use v_E to denote the constant production within the epithelium. We remark here that the assumption of constant production rate of molecule within the epithelium is different from the actual production terms $\sum_{j=0}^{2} \mu_j C_j$ and $\sum_{j=0}^{2} \eta_j C_j$ in Eqs. **S1**-**S2**, in which the production depends on the spatial distribution of the cells, and therefore depends on z. However, since A is produced by all types of cells, if the production rate μ_j is the same for all cells (as taken in our model and simulations), by the relation $C_0 + C_1 + C_2 = 1$, the production of A will be uniform in space. As for G, which is only produced by C_1 and C_2, its production is nearly uniform as C_2 constitutes the majority of the epithelium (in our simulation results, C_2 is usually larger than 0.8). Together, the production of the molecule can be approximated by a constant in those cases.

With those assumptions, the distribution of a at steady state is governed by the following equations:

$$
\begin{cases}
0 = D_E \dfrac{d^2 a}{dz^2} + v_E - k_E a, & \text{if } 0 < z < z_{max} \\[2ex]
0 = D_S \dfrac{d^2 a}{dz^2} - k_S a, & \text{if } z \le 0
\end{cases}
$$

If the continuity of $a(z)$ and $\dfrac{da(z)}{dz}$ are imposed at $z = 0$, we obtain the solution

$$
a(z) =
\begin{cases}
2v_E - \dfrac{2v_E \cosh\left(\lambda_E (z + z_{max})\right)}{\cosh\left(\lambda_E z_{max}\right) + \rho \sinh\left(\lambda_E z_{max}\right)}, & \text{if } 0 < z < z_{max} \\[3ex]
\dfrac{2e^{\frac{\lambda_E z}{\rho}} v_E \rho \sinh\left(\lambda_E z_{max}\right)}{\cosh\left(\lambda_E z_{max}\right) + \rho \sinh\left(\lambda_E z_{max}\right)}, & \text{if } z \le 0
\end{cases}
$$

where $\rho = \dfrac{\lambda_E}{\lambda_S}$, with $\lambda_E = \sqrt{k_E / D_E}$, $\lambda_S = \sqrt{k_S / D_S}$. λ_E and λ_S are length constants (with units of length^{-1}) and represent the inverse of decay lengths of a in the epithelium and stroma respectively. By taking derivatives, we obtain $a'(0)/a(0) = \rho = \lambda_S / \lambda_E$. This implies that *the*

permeability coefficient at the basal lamina, defined as $a'(0)/a(0)$, is the ratio of the decay lengths of molecule a in the epithelium and stroma.

C. Uptake of *A* by *F* (leaky boundary condition for *A* in Eq. 8) prevents extinction of the stem cell population

In this section, we use the steady state equations of *A*, along with its boundary conditions, to show how the leakiness of *A* from the epithelium to stroma affects the local dynamics of stem cell density, which in turn affects the global behavior of the system.

Consider Eqs. **1**-**5** and the quasi-steady-state approximation of *A* (Eq. **S3** and **S5**). We first take integration of Eq. **S3** over $[0, \overline{z}_{max}]$, where $\overline{z}_{max}$ denotes the epithelium thickness z_{max} at time $\overline{t}$. Using the leaky boundary condition Eq. **S5** at $z = 0$ and the no-flux boundary condition at $z = \overline{z}_{max}$, we get

$$0 = -D_A \alpha_1 [A]\big|_{z=0} + \sum_{j=0}^{2} \mu_j \int_0^{\overline{z}_{max}} C_j \, dz - a_{deg} \int_0^{\overline{z}_{max}} [A] \, dz, \qquad \text{[S15]}$$

By Eq. **S15** and the positivity of the term $a_{deg} \int_0^{\overline{z}_{max}} [A] \, dz$, we get the following inequality:

$$D_A \alpha_1 [A]\big|_{z=0} < \sum_{j=0}^{2} \mu_j \int_0^{\overline{z}_{max}} C_j \, dz, \qquad \text{[S16]}$$

Inequality **S16**, along with the formula for regulated replication probability of stem cells in Eq. **5**, gives rise to a lower bound for the replication probability of stem cell at $z = 0$:

$$p_0(0,t) = \frac{\overline{p}_0}{1 + (\gamma_A [A])^2} > \frac{\overline{p}_0}{1 + \left(\dfrac{\gamma_A}{D_A \alpha_1} \displaystyle\sum_{j=0}^{2} \mu_j \int_0^{\overline{z}_{max}} C_j \, dz \right)^2}. \qquad \text{[S17]}$$

Because $\overline{p}_0$ is greater than 0.5, we can write $\overline{p}_0$ as $0.5 + \varepsilon$, with $\varepsilon > 0$. Substituting $\overline{p}_0$ by $0.5 + \varepsilon$ in Eq. **S17**, and then by Eq. **1**, one obtains a lower bound for the overall proliferation rate of the stem cell $v_0(2p_0 - 1)$ at $z = 0$:

$$v_0 \left(2p_0(0,t) - 1 \right) > v_0 \frac{2\varepsilon - \left(\dfrac{\gamma_A}{D_A \alpha_1} \displaystyle\sum_{j=0}^{2} \mu_j \int_0^{\overline{z}_{max}} C_j \, dz \right)^2}{1 + \left(\dfrac{\gamma_A}{D_A \alpha_1} \displaystyle\sum_{j=0}^{2} \mu_j \int_0^{\overline{z}_{max}} C_j \, dz \right)^2} \qquad \text{[S18]}$$

According to inequality **S18**, as long as $\left(\dfrac{\gamma_A}{D_A \alpha_1} \displaystyle\sum_{j=0}^{2} \mu_j \int_0^{\overline{z}_{max}} C_j \, dz \right)^2 < 2\varepsilon$, $2p_0(0,t) - 1$ becomes positive, and hence $\dfrac{\partial C_0}{\partial t}(0,t) = v_0 (2p_0 - 1) C_0 > 0$. As a result, the stem cell density C_0 near the basal lamina starts to increase. In conclusion, when the system is close to an extinction state with $C_0 = C_1 = C_2 = 0$ for all z, the quantity $\displaystyle\sum_{j=0}^{2} \mu_j \int_0^{\overline{z}_{max}} C_j \, dz$ becomes close to zero, leading to an

increase in stem cell density near the basal lamina. This implies that *the system will never reach the extinction state* $C_0 = C_1 = C_2 = 0$.

D. Parameter sensitivity for Fig. 3, Fig. 5 and Fig. 6; parameter sensitivity for a_{deg} and g_{deg}

We find that the qualitative behavior and results demonstrated by Fig. 3, Fig. 5 and Fig. 6 are robust to parameter changes in the system. Fig. S2-S4 are examples of the corresponding dynamics of Fig. 3, 5 and 6 using different parameters from those figures. The parameters are randomly chosen from ranges around the values of the parameter used in Fig. 3, 5 and 6.

In Fig. S5, three values of a_{deg}, g_{deg} and f_{deg} ($5\times10^{-4}, 10^{-4}, 5\times10^{-5}$) are tested. It is found that the qualitative behavior with those parameters is similar to that with the typical value $a_{\text{deg}} = g_{\text{deg}} = f_{\text{deg}} = 10^{-3}$ used for all the other figures.

III. TABLES FOR PARAMETERS USED IN ALL FIGURES

Table S1. Parameters typically used for Fig. 1-6 and Fig. S1-S5 unless otherwise specified.

Parameters	Values	Units
$\overline{v}_0, \overline{v}_1$	1	per cell cycle
d_2	0.01	per cell cycle
D_A, D_G, D_F	10^{-7}	$cm^2 s^{-1}$
$\mu_0, \mu_1, \mu_2, \eta_1, \eta_2$	1×10^{-3}	$s^{-1}\mu M$
$a_{\text{deg}}, g_{\text{deg}}, f_{\text{deg}}$	1×10^{-3}	s^{-1}
ρ_F	150	$cm^{-1}\mu M$

Table S2: Parameters used in Fig. 3-6. '—' means not applicable.

Parameter	γ_A (μM^{-1})	γ_G (μM^{-1})	$\overline{p}_0$	$\overline{p}_1$	α_A, α_G (cm^{-1})	β (μM^{-1})	k_{af}, k_{gf} ($\mu M^{-1}s^{-1}$)
Fig. 3A	1.1	5	0.7	0.4	--	--	--
Fig. 3B	0.675~1.12	40	0.7	0.4	--	--	--
Fig. 3C	0.675~1.12	40	0.7	0.4	--	--	--
Fig. 3D	0.675~1.12	40	0.7	0.4	--	--	0
Fig. 4C (Fig. 4A, 4B case 1)	3	40	0.7	0.4	100	--	100
Fig. 4D (Fig. 4A, 4B case 2)	1.95	30	0.7	0.4	10	--	100
Fig. 4E (Fig. 4A, 4B case 3)	1.04	30	0.7	0.4	100	--	0
Fig. 5	3.9	40	0.7	0.4	100	--	10
Fig. 6	3.9	40	0.7	0.4	100	3	10

Table S3: Parameters used in Fig. S1-S5. '—' means not applicable.

Parameter	γ_A (μM^{-1})	γ_G (μM^{-1})	$\bar{p}_0$	$\bar{p}_1$	α_A, α_G (cm^{-1})	β (μM^{-1})	k_{af}, k_{gf} ($\mu M^{-1}s^{-1}$)	K_A, K_G (μM)	$a_{deg}, g_{deg}, f_{deg}$ (s^{-1})
Fig.S1A	0.85	7	0.7	0.4	100	--	--	0.5	--
Fig.S1B	2.62	7	0.7	0.4	100	--	--	0.5	--
Fig. S2A	1.4	3	0.8	0.3	--	--	--	--	--
Fig. S2B	0.9	6	0.6	0.5	--	--	--	--	--
Fig. S3A	2.73	40	0.7	0.4	32	--	10	--	--
Fig. S3B	5	20	0.8	0.3	100	--	100	--	--
Fig. S4A	2.73	40	0.7	0.4	32	3	10	--	--
Fig. S4B	5	20	0.8	0.3	100	3	100	--	--
Fig. S5A	1.6	25	0.7	0.4	100	--	10	--	5×10^{-4}
Fig. S5B	0.6	5	0.7	0.4	100	--	10	--	1×10^{-4}
Fig. S5C	0.47	3	0.7	0.4	100	--	100	--	5×10^{-5}

** In Fig.S1B, $\mu_0, \mu_1, \mu_2 = 5\times10^{-4}$.

REFERENCES

1. Briggs, W. L., V. E. Henson, and S. F. McCormick. 2000. A multigrid tutorial. Society for Industrial and Applied Mathematics, Philadelphia, PA.
2. Lo, W. C., C. S. Chou, K. K. Gokoffski, F. Y. M. Wan, A. D. Lander, A. L. Calof, and Q. Nie. 2009. Feedback regulation in multistage cell lineages. Mathematical Biosciences and Engineering 6:59-82.
3. Lander, A. D., K. K. Gokoffski, F. Y. M. Wan, Q. Nie, and A. L. Calof. 2009. Cell lineages and the logic of proliferative control. Plos Biology 7:84-100.
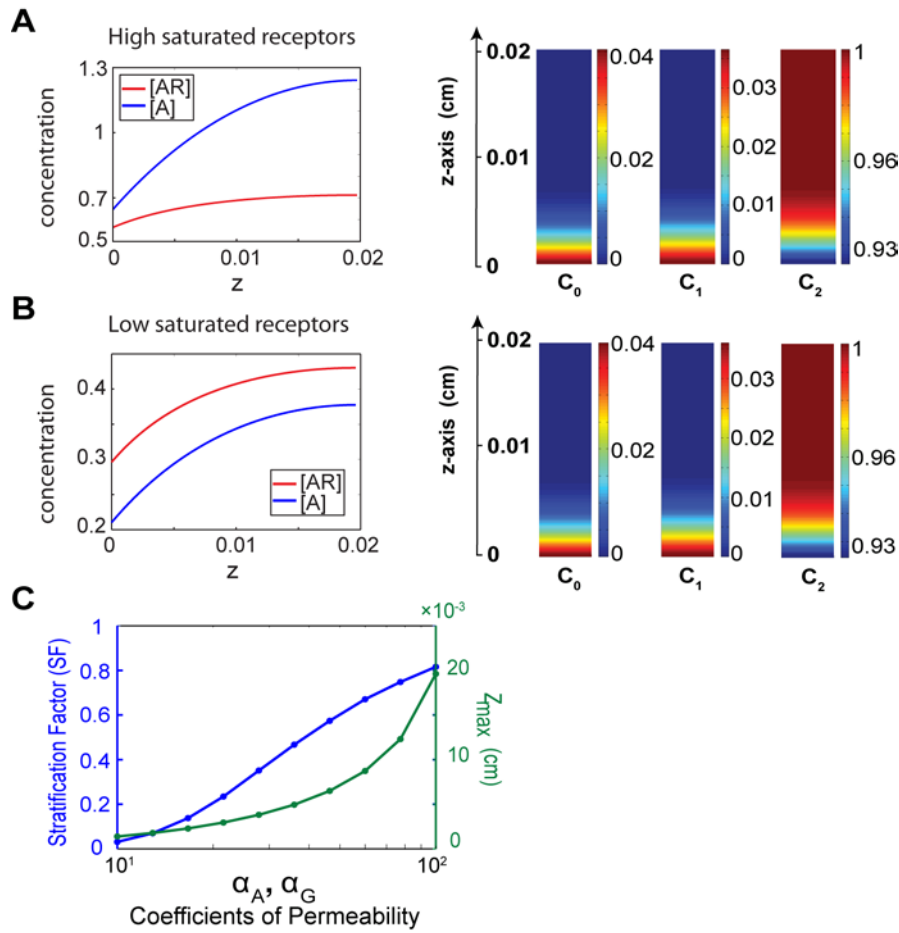
Figure S1

Figure S1. Tissue stratification and morphogen distribution with high and low saturated receptors. The parameters are listed in Tables S1 and S3. (A) Highly saturated case. Left panel: spatial distributions of ligand-bound receptors [AR] (red) and free molecules [A] (blue); right panel: cell distribution. (B) Low saturated case. Left panel: spatial distributions of [AR] (red) and [A] (blue); right panel: cell distribution. In the simulations of (A) and (B), z_{max} is fixed to be 0.02 cm, which can be achieved by adjusting one of γ_A, γ_G. (C) Correlation between permeability coefficients α_A, α_G with SF of stem cell and z_{max}; blue: permeability coefficients α_A, α_G in Eq. **8** (log scale) versus stratification factor (SF) defined in Eq. **9**; green: permeability coefficients versus epithelium thickness.
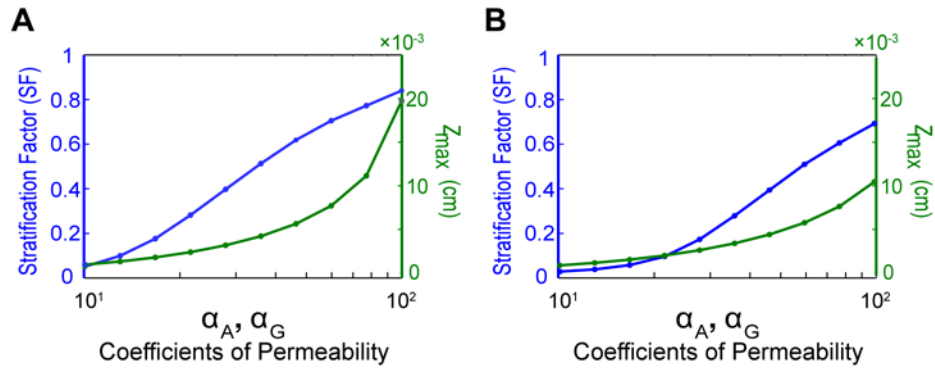
Figure S2.

Figure S2. Supporting calculations for Fig. 3A: correlation between permeability coefficients α_A, α_G with *SF* of stem cell and z_{max}, using two different sets of parameters for γ_A, γ_G, $\overline{p}_0$ and $\overline{p}_1$ (see Tables S1 and S3). The behavior of *SF* and z_{max} is similar to Fig. 3A: the epithelium thickness and stratification increases as the permeability coefficients of *A* and *G* are increased.
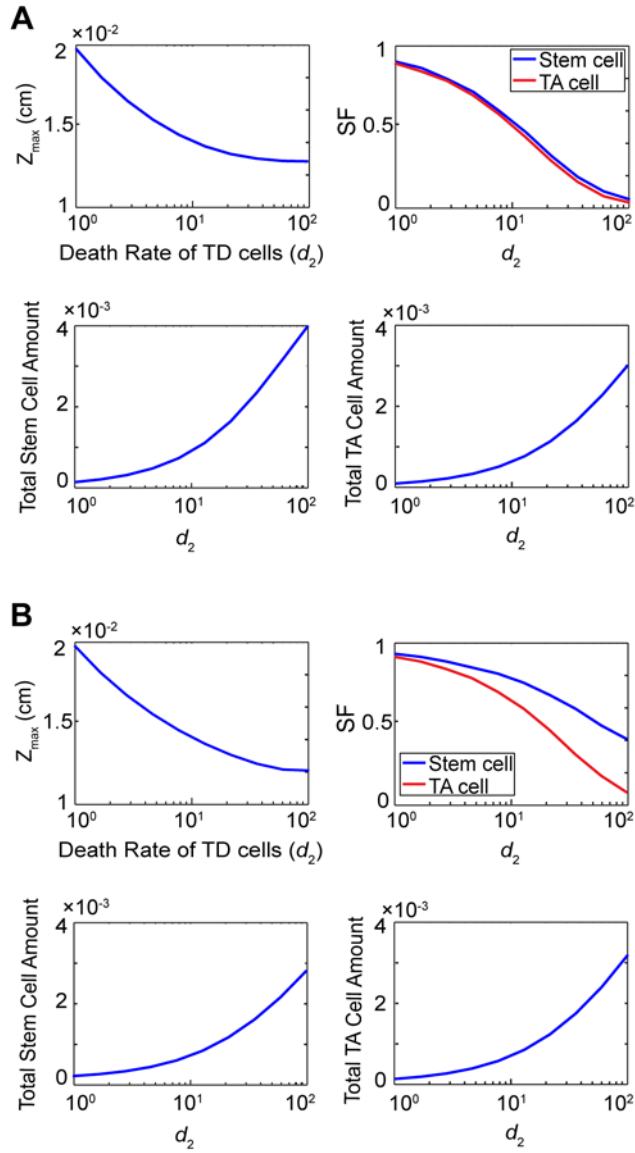
Figure S3.

Figure S3. Supporting calculations for Fig. 5: tissue stratification and thickness as functions of death rate of TD cells. Two sets of parameters are randomly chosen and used to conduct the same simulations as for Fig. 5. Parameters used in (A) are different from the original parameters for Fig. 5 in γ_A, α_A, α_G; parameters used in (B) are different from the original parameters for Fig. 5 in γ_A, γ_G, $\bar{p}_0$, $\bar{p}_1$, k_{af} and k_{gf}. The values of the parameters are listed in Tables S1 and S3. The behaviors of z_{max}, total stem/TA cell amount, and stem/TA cell stratification versus the death rate of TD cells are similar to Fig. 5.
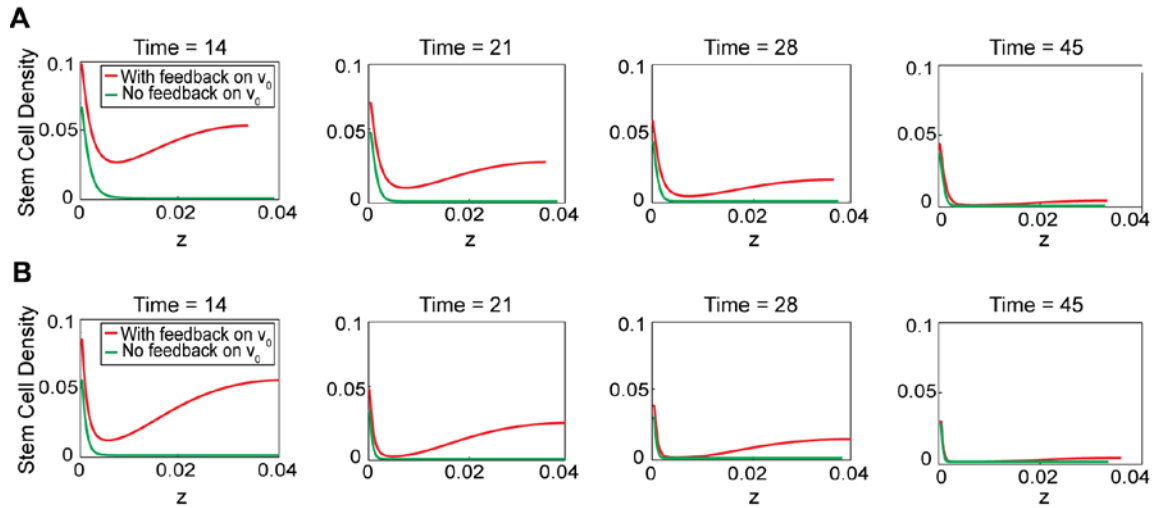
Figure S4.

A

B

Figure S4. Supporting calculations for Fig. 6: feedback on cell cycle length of stem cells induces transient peaks of stem cell density. Two sets of parameters are randomly chosen to conduct the same simulations as for Fig. 6. Parameters used in (A) are different from the original parameters for Fig. 6 in γ_A, α_A, α_G; parameters used in (B) are different from the original parameters for Fig. 6 in γ_A, γ_G, $\bar{p}_0$, $\bar{p}_1$, k_{af} and k_{gf}. The values of the parameters are listed in Tables S1 and S3. Similar to Fig. 6, the feedback on cell cycle length of stem cells induces transient peaks of stem cell density at the basal lamina and apical surface, and the peak at the apical end vanishes eventually.
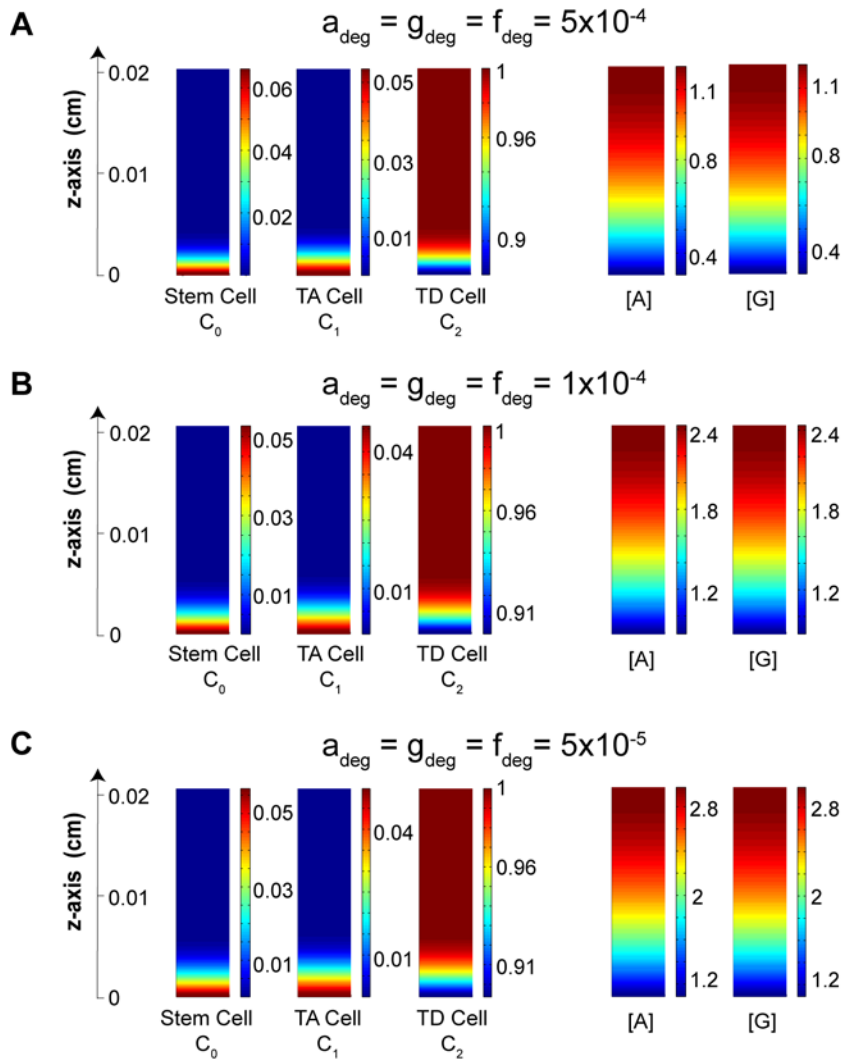
Figure S5.

Figure S5. Supporting calculations for different values of a_{deg}, g_{deg} and f_{deg}. (A) $a_{\text{deg}} = g_{\text{deg}} = f_{\text{deg}} = 5 \times 10^{-4}$; (B) $a_{\text{deg}} = g_{\text{deg}} = f_{\text{deg}} = 10^{-4}$; (C) $a_{\text{deg}} = g_{\text{deg}} = f_{\text{deg}} = 5 \times 10^{-5}$. In (A)-(C), parameters γ_A, γ_G are adjusted accordingly, and all the other parameters are listed in Tables S1 and S3.